# Structure and Surface Complexation at the Calcite(104)−Water Interface

Frank Heberling,* Tin Klačić, Paolo Raiteri, Julian D. Gale, Peter J. Eng, Joanne E. Stubbs, Teba Gil-Díaz, Tajana Begović, and Johannes Lützenkirchen

ABSTRACT: Calcite is the most stable polymorph of calcium carbonate ($CaCO_3$) under ambient conditions and is ubiquitous in natural systems. It plays a major role in controlling pH in environmental settings. Electrostatic phenomena at the calcite−water interface and the surface reactivity of calcite in general have important environmental implications. They may strongly impact nutrient and contaminant mobility in soils and other subsurface environments, they control oil recovery from limestone reservoirs, and they may impact the safety of nuclear waste disposal sites.

Besides the environmental relevance, the topic is significant for industrial applications and cultural heritage preservation. In this study, the structure of the calcite(104)−water interface is investigated on the basis of a new extensive set of crystal truncation rod data. The results agree with recently reported structures and resolve previous ambiguities with respect to the coordination sphere of surface Ca ions. These structural features are introduced into an electrostatic three plane surface complexation model, describing ion adsorption and charging at the calcite−water interface. Inner surface potential data for calcite, as measured with a calcite single crystal electrode, are used as constraints for the model in addition to zeta potential data. Ion adsorption parameters are compared with molecular dynamics simulations. All model parameters, including protonation constants, ion binding parameters, and Helmholtz capacitances, are within physically and chemically plausible ranges. A PhreeqC version of the model is presented, which we hope will foster application of the model in environmental studies.

KEYWORDS: calcite, mineral−water interface, surface−structure/−potential/−charge, crystal truncation rods, single crystal electrode, zeta potential, surface complexation model, molecular dynamics simulation
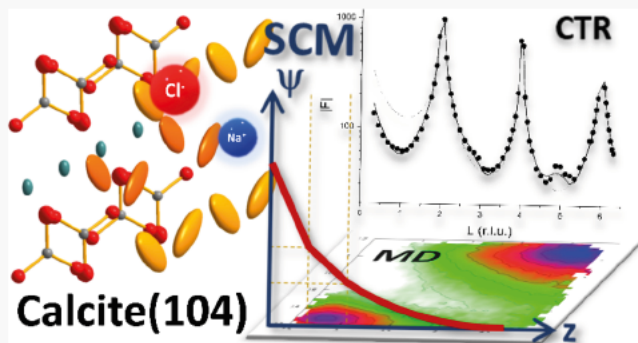
INTRODUCTION

Calcite is the most stable polymorph of calcium carbonate ($CaCO_3$) under ambient conditions[1] and one of the most abundant minerals in the Earth's crust.[2] Whenever present, calcite plays a major role in controlling the pH of soils and sediments, ground and surface waters, and even the oceans. Through sorption, recrystallization, (co)precipitation, and dissolution reactions, calcite influences the behavior of nutrients and contaminants in soils, sediments, and water bodies. Surface complexation reactions and concomitant charging phenomena at calcite−water interfaces represent important details with respect to the environmental reactivity of calcite. For example, they may have a direct impact on rock weathering.[3] Moreover, they affect the wetting behavior of calcite with respect to crude oil and are therefore crucial for oil recovery from limestone reservoirs[4] and its environmental implications. In the surroundings of nuclear waste disposal sites, calcite is a major constituent of clay formations considered as potential host rocks and a fracture filling material in potential granitic host rocks. Thus, calcite may sequester radionuclides and thereby impact their

dispersion from the waste after canister failure.[3−6] Calcite charging phenomena influence, for example, colloidal particle−particle interactions, which are of importance in the cement ,[7] paper , and other calcite (or limestone) processing industries as well as for cultural heritage preservation and restoration applications.

Numerous investigations of charging at the calcite−water interface and corresponding surface complexation models (SCMs) have been published over the past several decades, ranging from initial constant capacitance models[8−10] via our previous Basic Stern models[7,11−13] to elaborate three plane models (TPMs).[14−16] In this study, we revisit the molecular scale structure at the calcite(104)−water interface by means of

crystal truncation rod (CTR) data and compare the experimentally determined Debye−Waller parameters with computational predictions obtained from molecular dynamics (MD) simulations. (Inner)Surface potential data for the calcite−water interface, as measured with a calcite single crystal electrode (SCrE), are also presented. New surface potential and previous zeta potential data,[11] measured in the Na−Cl−Ca−C−H₂O system under, or close to, equilibrium conditions over a wide range of environmentally relevant conditions, are used to parameterize an electrostatic TPM. The model is kept as simple as possible in order to constrain the number of adjustable parameters and to enable application of the model in common speciation codes. To this end, a PhreeqC implementation of the model is provided. Most model parameters are justified on the basis of structural details, e.g., via the MUSIC equation,[17] by comparison with thermodynamic data for aqueous complexes as well as by comparing the ion binding constants obtained with those predicted by MD simulations using both rigid ion and polarizable force fields. With this new model, we present an SCM for calcite in which all parameters are within physically and chemically plausible ranges. Indeed, the main objective of the manuscript is to present a new SCM for calcite that offers a realistic representation of ion interactions at the calcite−water interface and is readily applicable for future environmental studies.

MATERIALS AND METHODS

Equilibrium solutions of calcite were prepared as previously described.[11] In brief, equilibrium compositions were calculated using PhreeqC (Version 3)[18,19] and the PSI/Nagra thermodynamic database (PSINA.dat[20]). Solutions were stirred and percolated with air until the expected equilibrium pH was reached. pH was measured using Orion Ross semi micro glass pH electrodes, which were calibrated against at least four Merck Titrisol buffer solutions. For CTR measurements, a 10 mmol/L RbBr solution was equilibrated with calcite and air (pH 8.2). The expected composition of this solution is shown in Table S1 (Supporting Information, SI) in the last column. The original aim of using RbBr was to enhance the X ray contrast of the background electrolyte ions compared to NaCl. However, upon comparison, no significant difference from the previous data measured in NaCl solution was observed. The only obvious difference was that the crystal surface prepared for these new measurements was considerably less rough, which led to increased diffracted intensities between the Bragg peaks (cf. (00L) CTRs depicted in the SI, Figure S1).

CTRs were recorded at the 13 ID C Beamline, Advanced Photon Source, (GSECARS, The University of Chicago). Measurements, data reduction, and structure refinement were performed as previously described.[11,21] The interfacial structure was optimized to minimize a weighted χ^2 function:

$$\chi^2 = 1/(n - p)\Sigma_i((F_{obs\_i} - F_{calc\_i})/F_{err\_i})^2,$$

where n is the number of data points (= 570); p is the number of adjustable parameters (= 66); the index i runs over all data points; and F_{obs}, F_{calc}, and F_{err} denote measured and calculated structure factor amplitudes and the related uncertainty, respectively. A section of the (−20L) CTR was measured repeatedly, as so called fiducial scans, before, throughout, and after the data collection in order to verify sample stability over the duration of the measurements. Symmetry equivalent CTRs ((0 ±1 L); (0 ±2 L)) were measured in order to assess the systematic uncertainty associated with the measurements.

MD simulations were used to compute the ion binding constants at infinite dilution for selected ions on the calcite basal plane in the presence of water. Multiple walker, well tempered metadynamics simulations using the PLUMED 2.7[22−26] plug in were used to determine the free energy profiles from which the ion binding constants were extracted. Unbiased MD simulations of electrolyte solutions were also used to assess the effect of finite concentrations. The atomic interactions were described using previously derived rigid ion (RigidFF) and polarizable AMOEBA force fields, which were both developed to accurately reproduce the thermodynamics of the ions in solution and the solubility of calcite.[27,28] All MD simulations with the RigidFF and AMOEBA force fields were performed with LAMMPS[29] and OpenMM,[30] respectively. Vibrational amplitudes for the water molecules adsorbed on the calcite surface, which are compared with interface structural Debye−Waller parameters from CTR analysis, were extracted from previously reported simulations[31] that used the same force fields. In the case of chloride adsorption, these classical MD simulations have also been complemented by *ab initio* molecular dynamics (AIMD) based on dispersion corrected density functional theory at the BLYP D3/TZV2P level in order to validate the likely existence, or not, of contact binding to the calcite surface. Full details of the simulation methods, including the models for the calcite water interface, are given in the SI.

Solutions for SCrE measurements were prepared with NaCl as the background electrolyte. Solution compositions for equilibrium measurements are reported in Table S1. SCrE measurements were performed in thermostat controlled vessels at 25.0 °C. During potentiometric SCrE titrations, solutions were stirred for 15 min after every solution addition. The stirrer was switched off during surface potential measurements. Acidimetric and alkalimetric titrations were carried out in 1 mmol/L NaCl solution with $HCl_{(aq)}$ and $NaOH_{(aq)}$, respectively. Experiments involving $CaCl_2$ and Na_2CO_3 addition were performed starting from 10 mmol/L NaCl solution at pH 10.0 ± 0.5. Non equilibrium measurements were performed under an Ar atmosphere.

An SCrE was built from a cleaved calcite single crystal (Iceland spar from Chihuahua, Mexico) with a size of approximately 5 mm × 5 mm × 1 mm. The natural Iceland spar crystals are chemically very pure and contain only minor amounts (<3000 ppm) of fluoride, chloride, and sulfur.[32] Sketches and images of the experimental setup for SCrE measurements and a short description of the measurement procedure are provided in the SI (Figure S2). SCrE potentials were measured against a reference electrode inside a combination glass pH−electrode (6.0234.100, Metrohm), which is immersed in the same solution and used for simultaneous pH measurements, as previously described.[33−35]

SCM development was based on PhreeqC.[19] The PhreeqPy wrapper around PhreeqC (www.phreeqpy.com) was combined with the optimization tool used for CTR interface structure refinement[21] to build new GUI based software, P³R (Python PhreeqC Parameter Refinement). This tool employs a simplex algorithm[36] for the optimization of chemical model parameters. It enables statistical parameter analyses similar to the USGS software UCODE.[37] The software developed here will be made available by the corresponding author upon request. Four layer model (FLM) calculations, similar to the recent implementation reported in Gil Diaz et al.,[38] were performed with a custom
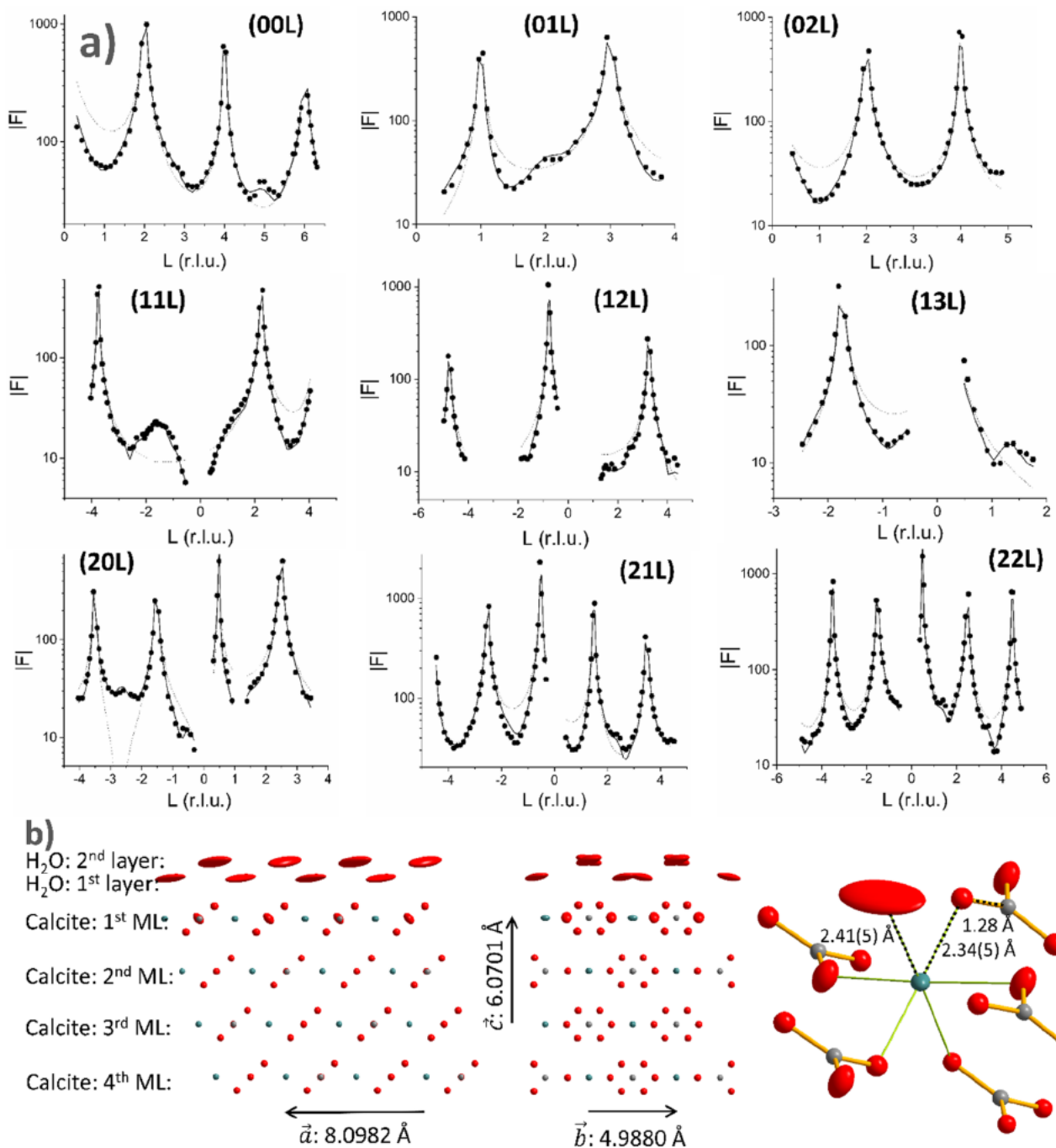
Figure 1. (a) CTR data (black circles), best fit model (solid black line), and bulk termination model (thin dashed line). Error bars on CTR data are smaller than the symbols (cf. also Figure S1). (b) Ball and stick representation of the best fit calcite–water interface structure (oxygen: red, carbon: gray, calcium: blue green). Note that hydrogen atoms of surface water molecules are not shown because X ray scattering measurements are not sensitive to hydrogen positions. Projections of the interface structure are along the surface crystallographic $\vec{b}$ (left) and $\vec{a}$ (middle) directions. These crystallographic orientations are related to the previously defined surface unit cell,[11] which transforms the calcite(104) plane (hexagonal system) into a (002) plane (pseudo monoclinic unit cell). The right image highlights the nearly perfect coordination octahedron around surface calcium ions. The dotted lines, annotated with bond distances, are the bond lengths relevant for MUSIC[17] calculations.

Python code, which was benchmarked against PhreeqC (cf. Figure S3).

RESULTS AND DISCUSSION

Interface Structure. The CTR data, model, and corre sponding best fit structure are depicted in Figure 1. A simplified version of a CIF file (all atoms, $P1$ symmetry) containing the interface structure, as depicted in Figure 1, is provided at the end

of the SI. Fiducial scans and symmetry equivalent CTRs are reported in the SI (Figures S4 and S5). The fiducial scans corroborate that the interface was stable and remained unaltered throughout the measurements. The symmetry equivalent CTRs indicate that there are negligible systematic errors. On the basis of these data, a constant relative error of 5% was assigned to the integrated structure factor amplitudes instead of relying on counting statistics for uncertainty estimation.
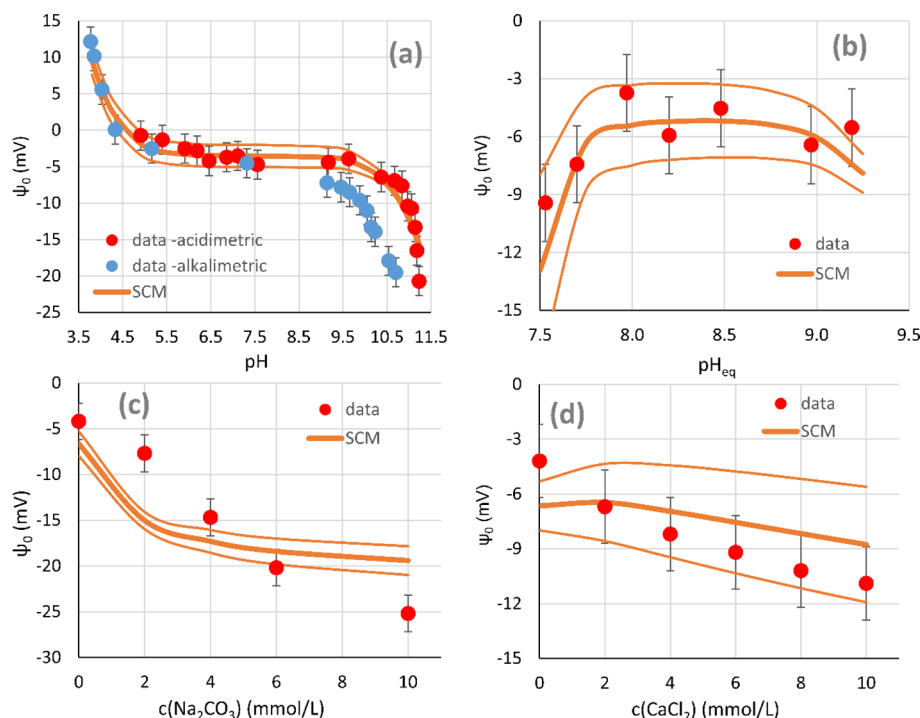
Figure 2. Inner surface potential data, as recorded with the calcite SCrE, and best fit model calculations. The confidence interval ($\pm 1\sigma$) for the SCM is indicated with thin solid lines. (a) Fast pH titration; no equilibrium with bulk calcite and atmosphere. The alkalimetric data was chosen as the best representation for low pH conditions. For high pH conditions, the acidimetric titration data was used. (b) pH_{eq} adjusted in separate suspensions to achieve equilibrium with calcite and atmospheric CO_2. (c, d) Na_2CO_3 and $CaCl_2$ addition experiments at pH 10.0 ± 0.5, respectively.

The model for the description of CTR data includes a fixed bulk calcite structure from the literature[39] and an interfacial calcite region with adjustable structural parameters, including four calcite monolayers (ML), similar to previous CTR studies.[40,41] Carbonate ions in the interfacial region are treated as rigid bodies, with three translational and three rotational degrees of freedom. Two adsorbed water molecules are explicitly included in the structural model above the calcite structure, i.e., H_2O 1 above the surface calcium atom and H_2O 2 above the outwardly oriented oxygen atom of the surface carbonate group, as suggested by previous SXRD studies[7,11,42−44] and simulation results.[15,31,40,45−48] Water molecules have to be approximated as oxygen atoms because hydrogen does not contribute to the CTR signal due to its low X ray scattering cross section. Beyond the adsorbed water, a semi infinite, laterally structureless, water profile was included in the model to account for scattering from bulk water.

Since the investigated calcite cleavage face had negligible roughness, no roughness model was applied (beta = 0).[49] Best fit parameters and the electron density profile across the adjusted calcite MLs, the adsorbed water, and the semi infinite bulk water profile are reported in Table S2 and Figure S6. The reference surface position for distances reported in the text is defined in terms of the z position of the surface calcium ions. The bulk water profile starts at 3.82 ± 0.03 Å above the surface and indicates an essentially structureless electron density, originating from bulk water. Adsorbed water molecules are arranged in two layers. First layer water molecules are located 2.34 ± 0.05 Å above the surface and 2.41 ± 0.05 Å away from the surface calcium ion, completing a close to ideal coordination octahedron (cf. Figure 1). For the first layer of water, the occupancy is fixed at 100%. Second layer adsorbed water molecules are located 3.29 ± 0.08 Å above the surface and 2.63

± 0.10 Å from the topmost oxygen atom of the surface carbonate ion. The occupancy for this water site is $67 \pm 15\%$. This water structure is in agreement with recent 3D CTR studies on calcite(104)[7,11,44] and simulation results.[40,44,46]

Among the four adjusted interfacial calcite MLs, the three lowest ones (2nd, 3rd, and 4th ML in Figure 1) show small relaxations of the ions from their bulk positions (<0.016 Å and mostly <0.005 Å). In the topmost calcite ML, the relaxation of ions from the bulk position is more pronounced (up to 0.034 Å). The surface carbonate ion is found to tilt $2.7° \pm 0.1°$ toward the surface calcium ion and to rotate $4.2° \pm 0.2°$ in the lateral directions. These rotations are slightly larger compared to the recent results of Brugman et al.[44] but comparable to our previous structure determination.[11] Debye−Waller factors in the topmost calcite layer are slightly increased compared to those in the bulk structure. Correspondingly, relaxations are only visible for the topmost calcite ML in Figure 1 and Figure S6. As a simple justification for the derived structure, bond valence sums according to Brown and Altermatt[50] are calculated for atoms in the structurally adjusted monolayers. They are all within $\pm 5\%$ of the nominal ion charges.

For the two adsorbed oxygen atoms (representing adsorbed water) as well as the Ca ion and the in plane oxygen atom of the carbonate ion in the topmost ML, anisotropic Debye−Waller factors were considered during adjustment. This led to an improved and more stable structure refinement with the weighted χ^2 of the best fit structure decreasing from 10 to 6. Thus, the improvement of the fit clearly outweighs the effect of the additional adjustable parameters. Anisotropic Debye−Waller factors are not yet routinely applied in surface structure refinements on the basis of CTR data, since this involves additional adjustable parameters (up to six per atom). Therefore, we compare the adjusted Debye−Waller factors
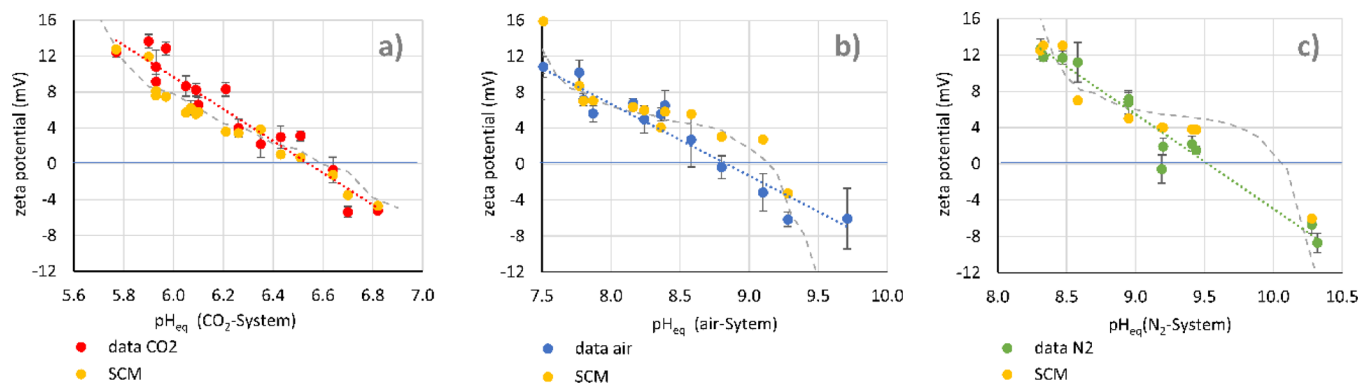
Figure 3. Zeta potential data at about 0.1 M ionic strength[11] (red, green, and blue dots) together with model fits for the best fit SCM (yellow dots). The gray dashed line highlights a generalized model prediction; the colored dashed lines are linear fits to the data. Panel (a) shows data in equilibrium with 1 bar CO_2; panel (b) shows data in equilibrium with atmospheric CO_2, $p(CO_2) = 10^{-3.44}$ bar; and panel (c) shows data in equilibrium with nitrogen gas, $p(CO_2) = 10^{-5.2}$ bar.
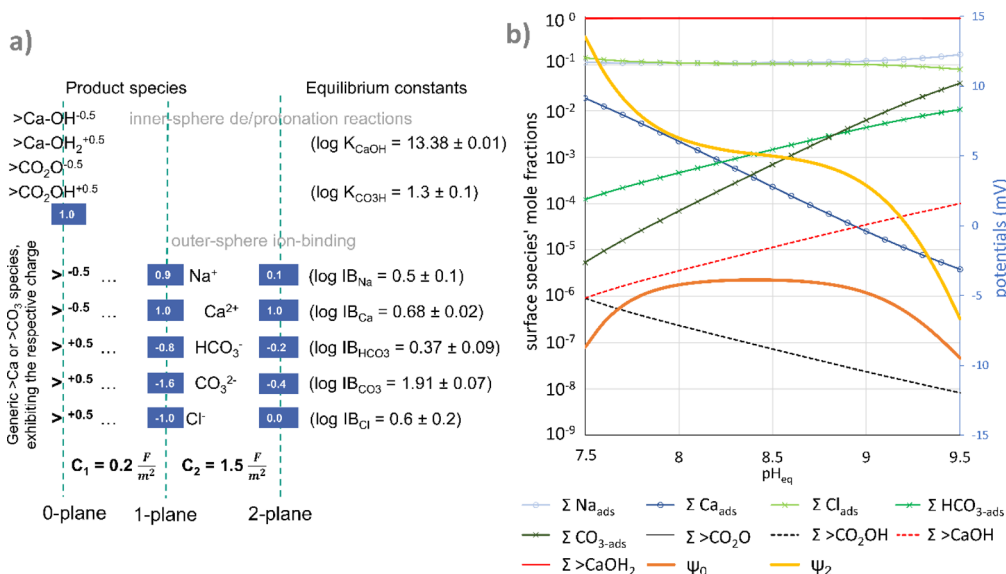

Figure 4. (a) Schematic and tabulated constants for the best fit SCM. Numbers in blue boxes denote CD parameters, specifying the distribution of charge between the planes of the TPM. (b) Speciation plot highlighting the abundance of inner sphere and adsorbed surface species (as mole fractions) and the corresponding potentials, ψ_0 and ψ_2, respectively. The simulation assumes 1 g/L calcite with a 1 m^2/g specific surface area in 0.1 M NaCl solution in equilibrium with calcite and atmospheric CO_2 ($p(CO_2) = 10^{-3.44}$ bar). HCl (pH < 8.3) or NaOH (pH > 8.3) are added to adjust the pH in the simulation.

with vibrational amplitudes derived from atom trajectories from previous MD simulations.[31] Corresponding parameters are reported in the SI (Table S3). For the two adsorbed water molecules, CTR and MD derived values compare well even on a quantitative level. Amplitudes for the surface Ca ions and the in plane oxygen atom are much smaller. While the average amplitudes are comparable, the shapes do not match well (cf. Figure 1 and Figure S7). Nevertheless, the improved stability of the refinements and the comparison with MD simulations seem to justify the use of anisotropic Debye−Waller factors in this surface structure refinement, especially for the adsorbed water molecules, where the resulting measured vibrational parameters (amplitudes and directions) seem to be in a realistic range.

From the interfacial structure, the bond distances indicated in Figure 1b (right) are used for MUSIC[17] calculations to estimate protonation constants of the surface functional groups, >Ca−$OH_2^{+0.5}$, and >$CO_2O^{-0.5}$, as described below. Crystallographic site densities of 4.95 nm^{-2} are applied in the SCM, and

knowledge regarding the thickness of the adsorbed water layer enables interfacial capacitance values to be constrained.

Inner Surface Potential. A major innovation in this study is the use of SCrE data to constrain the inner surface potential at the calcite(104) face during the adjustment of SCM parameters. The experimental data and model fits are shown in Figure 2. It is important to note that SCrE measurements provide only relative changes in the inner surface potential in relation to changes in the contact solution composition. During model adjustment, the model surface potential is modified by adjustable potential shifts applied to each experimental series. In Figure 2, the potential values are readjusted to the SCM ψ_0 in order to obtain an absolute value. Acidimetric and alkalimetric titrations under non equilibrium conditions are reported in Figure 2a. They show a broad plateau in surface potential at circumneutral pH, a steep decrease at pH > 10, and an increase at pH < 5. The alkalimetric data was chosen as the best representation for low pH conditions. These measurements start at low pH and therefore, data at high pH are significantly affected by calcite

dissolution. For high pH conditions, the acidimetric titration data were therefore considered during model adjustment. Addition of Na_2CO_3 at pH 10 ± 0.5 decreases the surface potential (Figure 2c) in line with previous assignments of CO_3^{2-} as a potential determining ion.[8−11,51] SCrE measured surface potentials at pH 10 ± 0.5 decrease upon addition of $CaCl_2$ (Figure 2d), which we interpret as an indication that the inner surface potential is more strongly influenced by Cl^- compared to Ca^{2+}. This was unexpected because Ca^{2+} has previously been considered to be the main potential determining ion for zeta potentials (here regarded as the 2 plane potential of the TPM).[11,51] It was difficult to accurately simulate the data from the Na_2CO_3 and $CaCl_2$ addition experiments. The general trends are, however, reproduced. The surface potential in equilibrium solutions as a function of pH (Figure 2b) is a complex interplay between all of the aforementioned effects. Potentials in equilibrium solutions remain essentially constant as a function of pH in the pH region investigated. Only at low pH a slight potential decrease is indicated. This is well reproduced by the model and reflects again the effect of adsorbing Cl^- originating from HCl addition for pH adjustment.

Zeta Potentials. Zeta potentials of calcite powder in equilibrium solutions at various pH values, equilibrated with atmospheres of various gases and CO_2 partial pressures, taken from our previous study[11] are shown together with model fits in Figure 3.

The model reproduces the increasing isoelectric points (IEP) with decreasing CO_2 partial pressure. The main factor controlling the zeta potential of calcite is the changing speciation of the solution with respect to Ca^{2+}, HCO_3^-, CO_3^{2-}, Na^+, and Cl^- concentrations as the equilibrium pH and CO_2 partial pressure are changed. Importantly, during the preparation of the solutions, the salt level was adjusted according to PhreeqC simulations in order to achieve a more or less constant ionic strength of 0.1 M (or for some datasets, 0.15 M) after addition of HCl or NaOH, dissolution of calcite, and equilibration with the gas phase.[11] Simulations are very sensitive to Na^+ and Cl^- concentrations. An example of a calculation with a constant background salt level is shown in Figure 4 for 0.1 M NaCl. The Figure also highlights the major model features. At high CO_2 partial pressure, the model is close to the experimental data and close to a linear trend, as indicated by the red dashed line in Figure 3a. The IEP is well reproduced. At lower CO_2 partial pressures (Figure 3b,c), simulations trace the S shaped surface potential function (Figure 2a), and simulated IEPs deviate slightly from the experimental data (up to ca. 0.5 pH units).

SCM Parameters. The SCM fits to the experimental data are displayed in Figures 2 and 3. Model parameters and a schematic of the model layout are presented in Figure 4a. Calcite surface speciation according to the new model is displayed along with calcite surface and 2 plane potentials (where the latter is taken as the zeta potential in this case) in Figure 4b. Model parameters are detailed in Table S4 (SI), which also contains information on how parameters were adjusted during model refinement. The most comprehensive description of the model and definition of the parameter usage are given by the example PhreeqC input provided toward the end of the SI document.

The goal behind this SCM was to provide an SCM that was as simple as possible, which offers a physically and chemically reasonable description of the processes at the calcite−water interface, and can be parameterized on the basis of reliable sets of experimental data. Accordingly, this SCM is different from those approaches trying to include a maximum of potentially relevant

reactions. The latter models may only be parameterized on the basis of theoretical input.[14−16] The present SCM is also quite different from our previous Basic Stern SCM,[7,11−13] which successfully simulated the complex conductivity evolution during calcite precipitation.[52] Differences compared to previous Basic Stern models mainly result from disregarding streaming potential data in the parameterization. The decision to omit these data was due to findings that the flow of non equilibrium solutions over surfaces affects the surface structure and potential in a complex way.[53−55] Since these studies indicate that measurements are influenced by kinetic processes during the flow of non equilibrium solutions over the surface, such data are not suitable for use in the parameterization of equilibrium models. Instead, SCrE data was included in the model parameterization. For these data, sufficient equilibration time is allowed and measurements are made during no flow (without stirring) conditions, and therefore kinetic effects remain negligible, while the solution conditions are sufficiently well defined during data acquisition.[54] Remarkably, the parameters that are solely adjusted to the SCrE potentiometric pH titration, namely, the surface protonation constants $K_{>CaOH}$ and $K_{>CO3H}$, coincide with MUSIC[17] estimates based on the interface structure as depicted in Figure 1 within the accuracy of the structure determination. The bond valence of the $>Ca-O(H_2O\ 1)$ bond with a 2.41 ± 0.05 Å length is 0.30 ± 0.05. Adding the contribution of a bound hydrogen atom (= 0.8) and a bridging hydrogen atom (= 0.2) leads to an overall bond valence sum of 1.30 ± 0.05 for the protonated oxygen in the $>CaOH^{-0.5}$ group. According to the MUSIC[17] model, the protonation reaction

$$>CaOH^{-0.5} + H^+ \rightleftharpoons\ >CaOH_2^{+0.5}$$
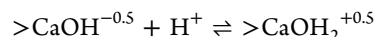
has a $\log_{10}K_{>CaOH} = 13.8 \pm 0.8$.

For the surface carbonate groups, $>CO_2O^{-0.5}$, two bond lengths need to be considered in the MUSIC calculation: the C−O bond with a fixed length of 1.28 Å (carbonate ions are treated as rigid bodies in the CTR model) and the Ca−O bond to the next surface >Ca ion (2.34 ± 0.05 Å, cf. Figure 1). Both bonds together lead to a bond valence sum of 1.72 ± 0.05. Adding the contribution of one hydrogen bonded hydrogen atom (= 0.2) leads to a bond valence sum of 1.92 ± 0.05, which results in the protonation reaction $>CO_2O^{-0.5} + H^+ \rightleftharpoons\ >CO_2OH^{+0.5}$ having $\log_{10}K_{>CO3H} = 1.3 \pm 1.0$. The respective best fit SCM parameters are 13.38 ± 0.01 and 1.3 ± 0.1.

The bond valence calculations may also be used to estimate the residual charge on the surface ions. In the present case, this leads to $>Ca^{+0.7}$ and $>CO_2O^{-0.3}$. However, as previously discussed in some detail,[7,11] use of the precise residual charges versus use of a generalized charge of ± 0.5 has only minor impacts on the model results, and the formal charges $>Ca^{+0.5}$ and $>CO_2O^{-0.5}$ allow for a simplified model formulation.

As shown in Figure 4b, these constants result in a surface that is dominated by unprotonated $>CO_2O^{-0.5}$ groups over the relevant pH range, and similarly, deprotonated water molecules (OH^-) in the adsorbed water layer are rare at pH ≤ 10, indicating a rather chemically inert surface. This may also explain why the calcite water interface structure appeared to be largely indifferent toward pH changes in previous interfacial structure determinations.[7,11,56] In return, this provides a justification to use the CTR data collected at pH 8.2 as the basis for a SCM covering a large pH range.
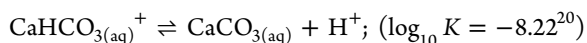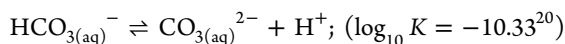
A justification for the physical and chemical plausibility of all parameters used in the SCM is possible. Capacitance values are 0.2 F/m^2 for the inner layer and 1.5 F/m^2 for the outer layer.

Based on previous findings, it seems reasonable that the inner layer,[11,31,56] where mainly protonation−deprotonation reactions occur, may be correlated with carbonate groups in the surface ML and the adsorbed, structured water layers. Water in this region shows a decreased relative permittivity close to the value of ice ($\varepsilon_{r1} = 6$). The thickness of this layer, z_1, is between 2 and 5 Å, depending on the definition of the boundary positions. Corresponding capacitance values ($C_1 = \varepsilon_0\varepsilon_{r1}/z_1$) should range from 0.1 to 0.3 F/m^2. $C_1 = 0.2$ F/m^2, thus, points either toward a slightly increased permittivity compared to ice or to a layer thickness on the lower side of the 2−5 Å range. On the other hand, $C_2 = 1.5$ F/m^2 for the outer layer points toward a water like relative permittivity ($\varepsilon_{r2} = 78.5$), which agrees with the relatively structureless bulk water profile beyond the adsorbed layers identified in the present and previous CTR studies[40,57] and MD simulations.[31,40,48]

The sodium binding constant ($\log_{10}$ IB$_{Na}$ = 0.5 ± 0.1) turned out to be the most critical parameter during SCM optimization. The upper limits for Rb$^+$ adsorption found in a previous RAXR investigation[58] were taken as an upper limit for Na$^+$ adsorption, assuming that the alkali metal ions behave similarly, as suggested by the CTR data. Na$^+$ surface coverage according to the SCM and the upper limits derived from RAXR[58] are depicted in Figure S8. The $\log_{10}$ IB$_{Na}$ = 0.5 ± 0.1 corresponds to about a 3% ML coverage at 10 mM NaCl and a 20% ML coverage at 100 mM NaCl in line with high resolution AFM investigations reporting direct observation of adsorbed Na$^+$ at the calcite(104) surface.[48] A further test of the plausibility of IB$_{Na}$ involves comparison with the aqueous ion pair formation constant. The $\log_{10}$ constant for the formation of NaCO$_3^-$ ion pairs in aqueous solution is 1.27.[20] It seems plausible that the binding of Na$^+$ to CO$_3^{2-}$ in the calcite surface ML, where the carbonate ion is already bound to five Ca^{2+} ions and only a small fraction of the ion charge is exposed to the solution, is considerably weaker. A similar argument can be made for Ca^{2+} adsorption. Here, the ion binding constant, $\log_{10}$ IB$_{Ca}$ = 0.68 ± 0.02, compares to a value of 3.23 for the $\log_{10}$ aqueous ion pair formation constant. The large difference in this case may be explained by the possibility of forming a contact ion pair in aqueous solution,[28] while at the calcite surface, outer sphere adsorption is expected.[11,31,48,56] The carbonate ion binding constant, $\log_{10}$ IB$_{CO3}$ = 1.91 ± 0.07, is even closer to the aqueous CaCO$_{3(aq)}$ ion pair formation constant. For bicarbonate adsorption, the relationship is similar. The $\log_{10}$ IB$_{HCO3}$ = 0.37 ± 0.09 at the surface compares to $\log_{10}$ K = 1.11 for the aqueous CaHCO$_3^+$ ion pair formation constant. The two ion binding constants, $\log_{10}$ IB$_{CO3}$ = 1.91 ± 0.07 and $\log_{10}$ IB$_{HCO3}$ = 0.37 ± 0.09, can be used to calculate a protonation constant for adsorbed carbonate:

$$>Ca - OH_2^{+0.5} \cdots HCO_3^- \rightleftharpoons >Ca - OH_2^{+0.5}$$
$$\cdots CO_3^{2-} + H^+; \ (\log_{10} K = -8.8 \pm 0.2).$$
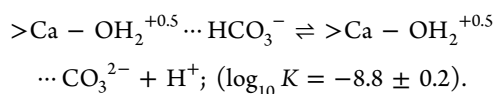
The value obtained is between the protonation constants for the free aqueous carbonate ion, and the calculated protonation constant for an aqueous CaCO$_3$ ion pair:

$$HCO_{3(aq)}^- \rightleftharpoons CO_{3(aq)}^{2-} + H^+; \ (\log_{10} K = -10.33^{20})$$

$$CaHCO_{3(aq)}^+ \rightleftharpoons CaCO_{3(aq)} + H^+; \ (\log_{10} K = -8.22^{20})$$

respectively, suggesting that adsorbed carbonate behaves more like Ca^{2+} ion paired aqueous carbonate. The Cl$^-$ ion binding constant is $\log_{10}$ IB$_{Cl}$ = 0.6 ± 0.2. Classical thermodynamic data

report a low CaCl$^+$ ion pair formation constant in aqueous solution, $\log_{10}$ K = −0.17.[59,60] Correspondingly, aqueous CaCl$^+$ ion pairing is not considered in the thermodynamic model being used.[20] However, recent findings report a higher value of $\log_{10}$ K = 0.5 ± 0.1,[61] comparable to Cl$^-$ binding to the calcite surface. In the SCM, the Cl$^-$ ion binding parameter is strongly correlated with the Na$^+$ ion binding constant. Once the Na$^+$ binding constant is fixed, it is, however, well constrained, especially by the CaCl$_2$ addition SCrE data (Figure 2d).

Another means of rationalizing ion binding constants is comparison with binding free energies from atomistic MD simulations. Two ways of calculating ion binding energies were evaluated from simulations using two different force fields as described in the SI, the rigid ion force field, RigidFF, and the AMOEBA polarizable force field. The resulting ion binding constants are reported in Table 1 (the same comparison in terms

Table 1. Comparison of Ion Binding Constants from the SCM with Corresponding Values Calculated from Adsorption Free Energies Extracted from MD Simulations via Metadynamics Calculations (metaD) or Ion Density Profiles of Unbiased MD Simulations (Density)

kJ/mol	experiment	RigidFF		AMOEBA	
	SCM	metaD	density	metaD	density
$\log_{10}$ IB$_{Na}$	0.5 ± 0.1	0.0	0.2	1.7	1.2
$\log_{10}$ IB$_{Ca}$	0.68 ± 0.02	0.0	0.0	1.7	1.2
$\log_{10}$ IB$_{HCO3}$	0.37 ± 0.09	0.0	0.2	0.9	0.7
$\log_{10}$ IB$_{CO3}$	1.91 ± 0.07	1.2	0.9	0.7	1.0
$\log_{10}$ IB$_{Cl}$	0.6 ± 0.2	0.7	0.2	0.3	0.5

of adsorption free energy is presented in the SI, Table S5). The full free energy profiles as a function of height above the surface are given in Figure 5. Figure S9 (SI) demonstrates the effect of the reweighing process used to obtain the graphs in Figure 5. A selection of ion density profiles above the surface obtained from simulations at a finite concentration is shown in the SI (Figure S10).

Ion binding constants extracted from AMOEBA MD simulations range from 0.3 < $\log_{10}$ IB < 1.7. They cover almost the same range as SCM ion binding constants (0.37 < $\log_{10}$ IB < 1.91). However, ion binding constants derived from RigidFF simulations are smaller, 0.0 < $\log_{10}$ IB < 1.2. RigidFF predicts the strongest ion binding for carbonate, which is in line with SCM ion binding constants. Accordingly, if we try to employ MD derived ion binding constants in the SCM (not shown), constants from RigidFF simulations perform slightly better than constants from AMOEBA simulations.

In RigidFF simulations, density profiles and adsorption free energies (Figures S10 and S11) indicate that ions, in general, stay beyond the two bound water layers at the calcite surface, which agrees with the concept of the SCM. Relative positions and amplitudes of the adsorption free energy minima, however, appear rather variable. AMOEBA predicts the strongest ion binding to occur for the cations Na$^+$ and Ca^{2+}, which come close to the surface and may even replace water above surface carbonate groups to form inner sphere species (cf. Figures S10 and S11).

In the case of Cl$^-$, AMOEBA and the reweighed metadynamics results with RigidFF predict a distinct local minimum for a contact ion state with the surface (Figure 5). Here, we can compare the 2D free energy landscape from MD with that obtained from AIMD (SI, Figures S12 and S13). In line
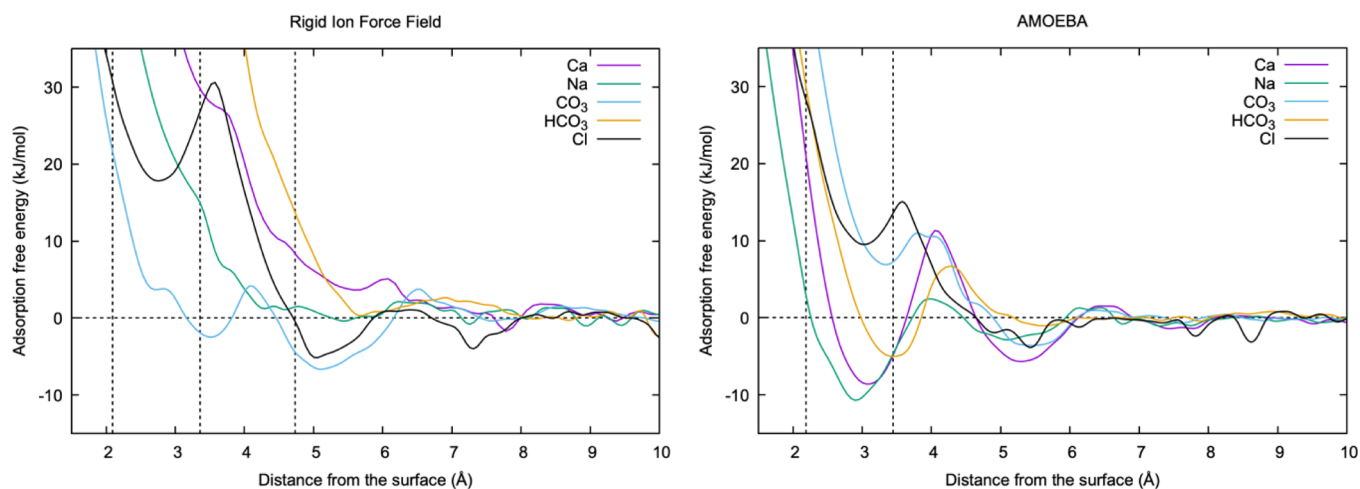
Figure 5. Free energy profiles for adsorption of ions on the hydrated basal surface of calcite as a function of height above the first layer of calcium ions as computed with RigidFF (left) and AMOEBA (right).

with AMOEBA, density functional theory suggests that Cl^- can indeed form a contact adsorption state with a surface calcium ion, with both methods agreeing that it lies ~10 kJ/mol or less above the solvent shared minimum, though RigidFF gives a value approximately double this. All methods after reweighing support the existence of a barrier for the contact state to dissociate, though the height varies substantially between approximately 5 and 30 kJ/mol.

The 2D free energy landscape for carbonate also shows a distinct local minimum for a contact adsorption state for RigidFF and AMOEBA. For bicarbonate, the case is less clear with RigidFF not even indicating a local minimum, while AMOEBA even predicts a global minimum in a contact adsorption state in a very similar position to that of the carbonate adsorption species.

The SCM CD parameters determine how ion charges are distributed over adjacent isopotential planes. Thus, they reflect the positioning of adsorbed ions between the hypothetical planes denoted 1 plane and 2 plane in Figure 4a. If a water like permittivity is considered between the 1 plane and 2 plane, as indicated by the capacitance value, the distance between the two planes should be roughly 5 Å (5×10^{-10} m ≈ ($78.5 \times 8.854 \times 10^{-12}/1.5$) m). CD parameters may thus be translated into ion positions: Cl^- at the 1 plane position, Na^+ 0.5 Å above the 1 plane, CO_3^{2-} and HCO_3^- 1 Å above the 1 plane, and Ca^{2+} 2.5 Å above the 1 plane. It should be kept in mind, however, that the absolute position of the hypothetical isopotential planes is arbitrary and the distance between the planes can only be a rough estimate. However, the relative positions of the ions between the planes are directly related to the data included in the model adjustment. For example, Cl^- mostly affecting the 0 plane potential adsorbs close to the surface in the 1 plane. In contrast, Ca^{2+} has only a minor influence on the 0 plane potential but is a potential determining ion for the 2 plane (i.e., zeta potential). Therefore, it adsorbs furthest away from the surface, halfway between the 1 plane and 2 plane. Here, the 2D free energy landscapes from AMOEBA seem to coincide with the CD parameters for the anions: Cl^- is getting slightly closer to the surface compared to carbonate and bicarbonate. If we accept this inner sphere contact adsorption state as the position of the 1 plane, then the contact adsorption state of Na^+ would also be close to the position derived from the CD parameters. However, the AMOEBA derived Ca^{2+} adsorption position and the relative

adsorption free energies clearly disagree with the experimental data. It is interesting to note that the SCM predicts such low ion surface coverages for the investigated solution compositions (< ca. 10% ML coverage) that a contact adsorption state for Na^+, Cl^-, HCO_3^-, and CO_3^{2-} (and Ca^{2+}) would not contradict previous CTR and RAXR studies.[11,56,58]

The ion distribution between the 1 and 2 planes, as implemented in the SCM via the CD parameters, follows the concept of a FLM. In a FLM, the Stern layer is subdivided by four planes (0−3), and three capacitances are considered between these planes. In a FLM for calcite, protons are adsorbed in the 0 plane, Cl^- in the 1 plane, and Ca^{2+} in the 2 plane. Na^+, CO_3^{2-}, and HCO_3^- are adsorbed between the 1 and 2 planes, and no specific ion adsorption is considered in the 3 plane such that the third capacitance is available to adjust the 3 plane potential with experimental zeta potentials. However, due to the limited availability of codes to calculate FLMs, we abandoned this approach and optimized the present TPM instead. For those interested, a FLM for calcite using the same protonation and ion binding constants, but with readjusted CD parameters and capacitances, is presented in the SI (Table S6 and Figure S14). In the FLM, the 0 plane and 3 plane potentials are more clearly separated, and tracing of the S shape of the 0 plane potential curve by the 3 plane potential as function of pH is not as pronounced. Furthermore, the FLM with the additional capacitance should be advantageous for adaption of the SCM to zeta potentials at varying ionic strengths.

In conclusion, and especially considering the model fits to the experimental data as shown in Figures 2 and 3, we are confident that the presented SCM provides a considerable improvement with respect to the thermodynamic description of the equilibrium surface speciation at the calcite−water interface compared to previous models. All SCM parameters are in chemically and physically plausible and realistic ranges. Thus, the model provides a parsimonious but realistic representation of surface complexation and ion adsorption processes at the calcite−water interface.

The interface structure determination largely confirms previous results.[11,40,44] The extensive CTR dataset, including the especially surface sensitive (11L) and (13L) CTRs, enables resolution of previous ambiguities with respect to the octahedral coordination environment of surface Ca groups, which can now be verified to be a close to ideal octahedron but was in some

previous works reported to be considerably distorted.[11,42,43] The resulting structure, including the anisotropic vibrational parameters for the hydration waters, may serve as a guide for simulation studies or the interpretation of high resolution AFM data.[62,63] For the first time, experimental SCrE inner surface potentials were included in the parameter optimization of a calcite SCM along with previous zeta potential data.[11] The newly developed three plane CD MUSIC SCM successfully describes even the unexpected trends ($CaCl_2$ addition data Figure 2d) in the SCrE data and the general course of the equilibrium zeta potential data. Data suspected to exhibit strong non equilibrium effects, such as streaming potential coupling coefficients,[11,13] or data obtained from measurements on potentially impure limestone samples,[51] were deliberately excluded from the parameter optimization. This should be kept in mind whenever the model is applied. Model parameters can be justified against MUSIC calculations, available thermodynamic data, and MD simulation results. Thus, compared to previous models, the model is considered as a strongly improved thermodynamic representation of surface complexation and ion adsorption processes at pure calcite—water interfaces under equilibrium conditions.

ASSOCIATED CONTENT

Supporting Information

The Supporting Information is available free of charge at https://pubs.acs.org/doi/10.1021/acs.est.1c03578.

Glossary of abbreviations and symbols, details on molecular dynamics simulations, supplementary CTR data and model parameters (Figures S1, S4, and S5—S7 and Tables S2 and S3), solution compositions for SCrE and CTR experiments (Table S1), sketches and photo graphs of the SCrE setup (Figure S2), benchmarking of the FLM code (Figure S3), supplementary details of the SCM (Tables S4 and S6 and Figures S8 and S14), supplementary details of molecular dynamics simulations (Figures S9—S13 and Table S5), PhreeqC type model input for the TPM, and cif file type structure information for the calcite—water interface structure (PDF)

AUTHOR INFORMATION

Corresponding Author

Frank Heberling — *Institute for Nuclear Waste Disposal, Karlsruhe Institute of Technology, 76021 Karlsruhe, Germany;* ⓞ orcid.org/0000 0002 2650 2071; Email: frank.heberling@kit.edu

Authors

Tin Klačić — *Division of Physical Chemistry, Department of Chemistry, Faculty of Science, University of Zagreb, HR 10000 Zagreb, Croatia*

Paolo Raiteri — *Curtin Institute for Computation/The Institute for Geoscience Research, School of Molecular and Life Sciences, Curtin University, Perth, WA 6845, Australia;* ⓞ orcid.org/ 0000 0003 0692 0505

Julian D. Gale — *Curtin Institute for Computation/The Institute for Geoscience Research, School of Molecular and Life Sciences, Curtin University, Perth, WA 6845, Australia;* ⓞ orcid.org/ 0000 0001 9587 9457

Peter J. Eng — *Center for Advanced Radiation Sources, The University of Chicago, Chicago, Illinois 60637, United States*

Joanne E. Stubbs — *Center for Advanced Radiation Sources, The University of Chicago, Chicago, Illinois 60637, United States;* ⓞ orcid.org/0000 0002 8509 2009

Teba Gil Díaz — *Institute for Nuclear Waste Disposal, Karlsruhe Institute of Technology, 76021 Karlsruhe, Germany; Institute of Geosciences, Friedrich Schiller Universität Jena, 07749 Jena, Germany*

Tajana Begović — *Division of Physical Chemistry, Department of Chemistry, Faculty of Science, University of Zagreb, HR 10000 Zagreb, Croatia;* ⓞ orcid.org/0000 0002 6670 6503

Johannes Lützenkirchen — *Institute for Nuclear Waste Disposal, Karlsruhe Institute of Technology, 76021 Karlsruhe, Germany;* ⓞ orcid.org/0000 0002 0611 2746

REFERENCES

(1) Plummer, L. N.; Busenberg, E. The solubilities of calcite, aragonite and vaterite in CO_2 H_2O solutions between 0 and 90[degree sign]C, and an evaluation of the aqueous model for the system $CaCO_3$ CO_2 H_2O. *Geochim. Cosmochim. Acta* 1982, *46*, 1011—1040.

(2) Morse, J. W.; Arvidson, R. S.; Luttge, A. Calcium carbonate formation and dissolution. *Chem. Rev.* 2007, *107*, 342—381.

(3) Heberling, F.; Brendebach, B.; Bosbach, D. Neptunium(V) adsorption to calcite. *J. Contam. Hydrol.* **2008**, *102*, 246−252.

(4) Heberling, F.; Denecke, M. A.; Bosbach, D. Neptunium(V) Coprecipitation with Calcite. *Environ. Sci. Technol.* **2008**, *42*, 471−476.

(5) Heberling, F.; Vinograd, V. L.; Polly, R.; Gale, J. D.; Heck, S.; Rothe, J.; Bosbach, D.; Geckeis, H.; Winkler, B. A thermodynamic adsorption/entrapment model for selenium(IV) coprecipitation with calcite. *Geochim. Cosmochim. Acta* **2014**, *134*, 16−38.

(6) Curti, E. Coprecipitation of radionuclides with calcite: estimation of partition coefficients based on a review of laboratory investigations and geochemical data. *Appl. Geochem.* **1999**, *14*, 433−445.

(7) Heberling, F.; Bosbach, D.; Eckhardt, J. D.; Fischer, U.; Glowacky, J.; Haist, M.; Kramar, U.; Loos, S.; Müller, H. S.; Neumann, T.; Pust, C.; Schäfer, T.; Stelling, J.; Ukrainczyk, M.; Vinograd, V.; Vučak, M.; Winkler, B. Reactivity of the calcite−water interface, from molecular scale processes to geochemical engineering. *Appl. Geochem.* **2014**, *45*, 158−190.

(8) Van Cappellen, P.; Charlet, L.; Stumm, W.; Wersin, P. A surface complexation model of the carbonate mineral aqueous solution interface. *Geochim. Cosmochim. Acta* **1993**, *57*, 3505−3518.

(9) Pokrovsky, O. S.; Mielczarski, J. A.; Barres, O.; Schott, J. Surface speciation models of calcite and dolomite/aqueous solution interfaces and their spectroscopic evaluation. *Langmuir* **2000**, *16*, 2677−2688.

(10) Pokrovsky, O. S.; Schott, J. Surface chemistry and dissolution kinetics of divalent metal carbonates. *Environ. Sci. Technol.* **2002**, *36*, 426−432.

(11) Heberling, F.; Trainor, T. P.; Lützenkirchen, J.; Eng, P.; Denecke, M. A.; Bosbach, D. Structure and reactivity of the calcite water interface. *J. Colloid Interface Sci.* **2011**, *354*, 843−857.

(12) Heberling, F.; Trainor, T. P.; Lützenkirchen, J.; Eng, P.; Denecke, M. A.; Bosbach, D. Corrigendum to "Structure and reactivity of the calcite−water interface" [J. Colloid Interface Sci. 354 (2011) 843−857]. *J. Colloid Interface Sci.* **2013**, 230.

(13) Li, S.; Leroy, P.; Heberling, F.; Devau, N.; Jougnot, D.; Chiaberge, C. Influence of surface conductivity on the apparent zeta potential of calcite. *J. Colloid Interface Sci.* **2016**, *468*, 262−275.

(14) Wolthers, M.; Charlet, L.; Van Cappellen, P. The Surface Chemistry of Divalent Metal Carbonate Minerals; a critical Aassess ment of Surface Charge and Potential Data unsing the Charge Distribution Multi Site Ion Complexation Model. *Am. J. Sci.* **2008**, *308*, 905−941.

(15) Wolthers, M.; Di Tommaso, D.; Du, Z.; de Leeuw, N. H. Calcite surface structure and reactivity: molecular dynamics simulations and macroscopic surface modelling of the calcite water interface. *Phys. Chem. Chem. Phys.* **2012**, *14*, 15145−15157.

(16) Wolthers, M.; Nehrke, G.; Gustafsson, J. P.; Van Cappellen, P. Calcite growth kinetics: Modeling the effect of solution stoichiometry. *Geochim. Cosmochim. Acta* **2012**, *77*, 121−134.

(17) Hiemstra, T.; Van Riemsdijk, W.; Bolt, G. Multisite proton adsorption modeling at the solid/solution interface of (hydr) oxides: A new approach: I Model description and evaluation of intrinsic reaction constants. *J. Colloid Interface Sci.* **1989**, *133*, 91−104.

(18) Appelo, C. A. J.; Parkhurst, D. L.; Post, V. E. A. Equations for calculating hydrogeochemical reactions of minerals and gases such as CO2 at high pressures and temperatures. *Geochim. Cosmochim. Acta* **2014**, *125*, 49−67.

(19) Parkhurst, D. L.; Appelo, C. Description of input and examples for PHREEQC version 3—a computer program for speciation, batch reaction, one dimensional transport, and inverse geochemical calcu lations. *US Geol. Surv. Tech. Methods* **2013**, *6*, 497.

(20) Thoenen, T.; Hummel, W.; Berner, U.; Curti, E., *The PSI/Nagra Chemical Thermodynamic Database 12/07*; Paul Scherrer Institut: Villigen PSI, Switzerland, 2014; Vol. *14 04*.

(21) Heberling, F.; Eng, P.; Denecke, M. A.; Lutzenkirchen, J.; Geckeis, H. Electrolyte layering at the calcite(104) water interface indicated by Rb+− and Se(vi) K edge resonant interface diffraction. *Phys. Chem. Chem. Phys.* **2014**, *16*, 12782−12792.

(22) Laio, A.; Parrinello, M. Escaping free energy minima. *Proc. Natl. Acad. Sci.* **2002**, *99*, 12562.

(23) Barducci, A.; Bussi, G.; Parrinello, M. Well Tempered Metadynamics: A Smoothly Converging and Tunable Free Energy Method. *Phys. Rev. Lett.* **2008**, *100*, 020603.

(24) Raiteri, P.; Laio, A.; Gervasio, F. L.; Micheletti, C.; Parrinello, M. Efficient Reconstruction of Complex Free Energy Landscapes by Multiple Walkers Metadynamics. *J. Phys. Chem. B* **2006**, *110*, 3533−3539.

(25) Bonomi, M.; Bussi, G.; Camilloni, C.; Tribello, G. A.; Banáš, P.; Barducci, A.; Bernetti, M.; Bolhuis, P. G.; Bottaro, S.; Branduardi, D.; Capelli, R.; Carloni, P.; Ceriotti, M.; Cesari, A.; Chen, H.; Chen, W.; Colizzi, F.; De, S.; De La Pierre, M.; Donadio, D.; Drobot, V.; Ensing, B.; Ferguson, A. L.; Filizola, M.; Fraser, J. S.; Fu, H.; Gasparotto, P.; Gervasio, F. L.; Giberti, F.; Gil Ley, A.; Giorgino, T.; Heller, G. T.; Hocky, G. M.; Iannuzzi, M.; Invernizzi, M.; Jelfs, K. E.; Jussupow, A.; Kirilin, E.; Laio, A.; Limongelli, V.; Lindorff Larsen, K.; Löhr, T.; Marinelli, F.; Martin Samos, L.; Masetti, M.; Meyer, R.; Michaelides, A.; Molteni, C.; Morishita, T.; Nava, M.; Paissoni, C.; Papaleo, E.; Parrinello, M.; Pfaendtner, J.; Piaggi, P.; Piccini, G.; Pietropaolo, A.; Pietrucci, F.; Pipolo, S.; Provasi, D.; Quigley, D.; Raiteri, P.; Raniolo, S.; Rydzewski, J.; Salvalaglio, M.; Sosso, G. C.; Spiwok, V.; Šponer, J.; Swenson, D. W. H.; Tiwary, P.; Valsson, O.; Vendruscolo, M.; Voth, G. A.; White, A.; The, P. c. Promoting transparency and reproducibility in enhanced molecular simulations. *Nat. Methods* **2019**, *16*, 670−673.

(26) Tribello, G. A.; Bonomi, M.; Branduardi, D.; Camilloni, C.; Bussi, G. PLUMED 2: New feathers for an old bird. *Comput. Phys. Commun.* **2014**, *185*, 604−613.

(27) Raiteri, P.; Demichelis, R.; Gale, J. D. Thermodynamically Consistent Force Field for Molecular Dynamics Simulations of Alkaline Earth Carbonates and Their Aqueous Speciation. *J. Phys. Chem. C* **2015**, *119*, 24447−24458.

(28) Raiteri, P.; Schuitemaker, A.; Gale, J. D. Ion Pairing and Multiple Ion Binding in Calcium Carbonate Solutions Based on a Polarizable AMOEBA Force Field and Ab Initio Molecular Dynamics. *J. Phys. Chem. B* **2020**, *124*, 3568−3582.

(29) Plimpton, S. Fast Parallel Algorithms for Short Range Molecular Dynamics. *J. Comput. Phys.* **1995**, *117*, 1−19.

(30) Eastman, P.; Swails, J.; Chodera, J. D.; McGibbon, R. T.; Zhao, Y.; Beauchamp, K. A.; Wang, L. P.; Simmonett, A. C.; Harrigan, M. P.; Stern, C. D.; Wiewiora, R. P.; Brooks, B. R.; Pande, V. S. OpenMM 7: Rapid development of high performance algorithms for molecular dynamics. *PLoS Comput. Biol.* **2017**, *13*, No. e1005659.

(31) Raiteri, P.; Gale, J. D.; Quigley, D.; Rodger, P. M. Derivation of an Accurate Force Field for Simulating the Growth of Calcium Carbonate from Aqueous Solution: A New Model for the Calcite Water Interface. *J. Phys. Chem. C* **2010**, *114*, 5997−6010.

(32) Heberling, F.; Paulig, L.; Nie, Z.; Schild, D.; Finck, N. Morphology Controls on Calcite Recrystallization. *Environ. Sci. Technol.* **2016**, *50*, 11735−11741.

(33) Klačić, T.; Tomić, M.; Namjesnik, D.; Pielić, B.; Begović, T. Mechanism of surface reactions and dissolution of fluorite surface in an aqueous electrolyte solution. *Environ. Chem.* **2019**, *16*, 529−540.

(34) Preočanin, T.; Namjesnik, D.; Brown, M. A.; Lützenkirchen, J. The relationship between inner surface potential and electrokinetic potential from an experimental and theoretical point of view. *Environ. Chem.* **2017**, *14*, 295−309.

(35) Preočanin, T.; Kallay, N. Evaluation of surface potential from single crystal electrode potential. *Adsorption* **2013**, *19*, 259−267.

(36) Nelder, J. A.; Mead, R. A Simplex Method for Function Minimization. *Comput. J.* **1965**, *7*, 308−313.

(37) Poeter, E. P.; Hill, M. C. *Documentation of UCODE, a computer code for universal inverse modeling*; US Geological Survey, 1998, 122.

(38) Gil Díaz, T.; Jara Heredia, D.; Heberling, F.; Lützenkirchen, J.; Link, J.; Sowoidnich, T.; Ludwig, H. M.; Haist, M.; Schäfer, T. Charge regulated solid liquid interfaces interacting on the nanoscale: Benchmarking of a generalized speciation code (SINFONIA). *Adv. Colloid Interface Sci.* **2021**, *294*, 102469.

(39) Markgraf, S. A.; Reeder, R. J. High Temperature Structure Refinements of Calcite and Magnesite. *Am. Mineral* **1985**, *70*, 590−600.

(40) Fenter, P.; Kerisit, S.; Raiteri, P.; Gale, J. D. Is the Calcite Water Interface Understood? Direct Comparisons of Molecular Dynamics Simulations with Specular X ray Reflectivity Data. *J. Phys. Chem. C* **2013**, *117*, 5028−5042.

(41) Fenter, P.; Sturchio, N. C. Calcite (1 0 4) water interface structure, revisited. *Geochim. Cosmochim. Acta* **2012**, *97*, 58−69.

(42) Magdans, U.; Torrelles, X.; Angermund, K.; Gies, H.; Rius, J. Crystalline order of a water glycine film coadsorbed on the (104) calcite surface. *Langmuir* **2007**, *23*, 4999−5004.

(43) Geissbuhler, P.; Fenter, P.; DiMasi, E.; Srajer, G.; Sorensen, L. B.; Sturchio, N. C. Three dimensional structure of the calcite water interface by surface X ray scattering. *Surf. Sci.* **2004**, *573*, 191−203.

(44) Brugman, S. J. T.; Raiteri, P.; Accordini, P.; Megens, F.; Gale, J. D.; Vlieg, E. Calcite (104) Surface−Electrolyte Structure: A 3D Comparison of Surface X ray Diffraction and Simulations. *J. Phys. Chem. C* **2020**, *124*, 18564−18575.

(45) Kerisit, S.; Parker, S. C. Free energy of adsorption of water and metal ions on the (1 0 1 4) calcite surface. *J. Am. Chem. Soc.* **2004**, *126*, 10152−10161.

(46) Polly, R.; Heberling, F.; Schimmelpfennig, B.; Geckeis, H. Quantum Chemical Investigation of the Selenite Incorporation into the Calcite (1014) Surface. *J. Phys. Chem. C* **2017**, *121*, 20217−20228.

(47) Villegas Jimenez, A.; Mucci, A.; Whitehead, M. A. Theoretical Insights into the Hydrated (10. 4) Calcite Surface: Structure, Energetics, and Bonding Relationships. *Langmuir* **2009**, *25*, 6813−6824.

(48) Ricci, M.; Spijker, P.; Stellacci, F.; Molinari, J. F.; Voïtchovsky, K. Direct Visualization of Single Ions in the Stern Layer of Calcite. *Langmuir* **2013**, *29*, 2207−2216.

(49) Robinson, I. K. Crystal truncation rods and surface roughness. *Phys. Rev. B* **1986**, *33*, 3830−3836.

(50) Brown, I. D.; Altermatt, D. Bond Valence Parameters obtained from a systematic analysis of the Inorganic Crystal Structure Database. *Acta Crystallogr., Sect. B: Struct. Sci.* **1985**, *41*, 244.

(51) Al Mahrouqi, D.; Vinogradov, J.; Jackson, M. D. Zeta potential of artificial and natural calcite in aqueous solution. *Adv. Colloid Interface Sci.* **2017**, *240*, 60−76.

(52) Leroy, P.; Li, S.; Jougnot, D.; Revil, A.; Wu, Y. Modelling the evolution of complex conductivity during calcite precipitation on glass beads. *Geophys. J. Int.* **2017**, *209*, 123−140.

(53) Lis, D.; Backus, E. H. G.; Hunger, J.; Parekh, S. H.; Bonn, M. Liquid flow along a solid surface reversibly alters interfacial chemistry. *Science* **2014**, *344*, 1138−1142.

(54) Preočanin, T.; Namjesnik, D.; Klačić, T.; Šutalo, P. The effects on the response of metal oxide and fluorite single crystal electrodes and the equilibration process in the interfacial region. *Croat. Chem. Acta* **2017**, *90*, 333−344.

(55) Lützenkirchen, J.; Scharnweber, T.; Ho, T.; Striolo, A.; Sulpizi, M.; Abdelmonem, A. A set up for simultaneous measurement of second harmonic generation and streaming potential and some test applications. *J. Colloid Interface Sci.* **2018**, *529*, 294−305.

(56) Fenter, P.; Geissbuhler, P.; DiMasi, E.; Srajer, G.; Sorensen, L. B.; Sturchio, N. C. Surface speciation of calcite observed in situ by high resolution X ray reflectivity. *Geochim. Cosmochim. Acta* **2000**, *64*, 1221−1228.

(57) Fenter, P.; Sturchio, N. C. Mineral water interfacial structures revealed by synchrotron X ray scattering. *Prog. Surf. Sci.* **2004**, *77*, 171−258.

(58) Lee, S. S.; Heberling, F.; Sturchio, N. C.; Eng, P. J.; Fenter, P. Surface Charge of the Calcite (104) Terrace Measured by Rb+ Adsorption in Aqueous Solutions Using Resonant Anomalous X ray Reflectivity. *J. Phys. Chem. C* **2016**, *120*, 15216−15223.

(59) Larentzos, J. P.; Criscenti, L. J. A Molecular Dynamics Study of Alkaline Earth Metal−Chloride Complexation in Aqueous Solution. *J. Phys. Chem. B* **2008**, *112*, 14243−14250.

(60) Majer, V.; Štulík, K. A study of the stability of alkaline earth metal complexes with fluoride and chloride ions at various temperatures by potentiometry with ion selective electrodes. *Talanta* **1982**, *29*, 145−148.

(61) Friesen, S.; Hefter, G.; Buchner, R. Cation Hydration and Ion Pairing in Aqueous Solutions of $MgCl_2$ and $CaCl_2$. *J. Phys. Chem. B* **2019**, *123*, 891−900.

(62) Reischl, B.; Raiteri, P.; Gale, J. D.; Rohl, A. L. Atomistic Simulation of Atomic Force Microscopy Imaging of Hydration Layers on Calcite, Dolomite, and Magnesite Surfaces. *J. Phys. Chem. C* **2019**, *123*, 14985−14992.

(63) Marutschke, C.; Walters, D.; Cleveland, J.; Hermes, I.; Bechstein, R.; Kühnle, A. Three dimensional hydration layer mapping on the (10.4) surface of calcite using amplitude modulation atomic force microscopy. *Nanotechnology* **2014**, *25*, 335703.